Ultrasonic-Assisted Synthesis of Zinc Borates: Effect of Boron Sources

[1]Fatma Tugce Senberber Dumanli, [2]Azmi Seyhun Kipcak, [2]Duygu Sena Vardar and [2]Nurcan Tugrul*
*[1]Nisantasi University, Neotech Campus, Faculty of Engineering and Architecture,
Department of Civil Engineering, Tasyoncasi Street No.1V and 1Y, Sariyer, Istanbul, Turkey.*
*[2]Yildiz Technical University, Davutpasa Campus, Faculty of Chemical and Metallurgical Engineering,
Department of Chemical Engineering, Davutpasa Street No.127, Esenler, Istanbul, Turkey.*
ntugrul@yildiz.edu.tr*

Summary: Sonochemistry meaning ultrasound-assisted chemistry plays an important role in the synthesis of inorganic compounds. Among these inorganic compounds, zinc borates are used for the flame-retarding agent. In this study using zinc chloride ($ZnCl_2$), boric acid (H_3BO_3), $Na_2B_4O_7 \cdot 10H_2O$, $Na_2B_4O_7 \cdot 5H_2O$ and NaOH as raw materials, a zinc borate compound in the formulae of $Zn_3B_6O_{12} \cdot 3.5H_2O$ was obtained using an ultrasonic probe. Crystal structures of samples were identified using X-ray diffraction (XRD). The symmetric and asymmetric stretching between boron and oxygen atoms were searched by Fourier-transform infrared (FT-IR) and Raman spectroscopies. The effects of boron sources on sample morphology were examined by scanning electron microscopy (SEM). From the results, it was seen that $Zn_3B_6O_{12} \cdot 3.5H_2O$ can easily be produced from these raw materials with the synthesis parameters of 80-90°C and 40-55 min. From the SEM results, it was seen that the minimum particle size obtained was 172 nm. Reaction efficiencies were calculated between 79.6 and $94.0 \pm 0.5\%$. Thermal feature of the obtained pure phase, investigated with the thermogravimetric analyses. The dehydration of the synthesized $Zn_3B_6O_{12} \cdot 3.5H_2O$ was seen between 262 and 413°C with a total mass loss of 13.25%.

Keywords: Zinc borate, Sonochemistry, X-Ray diffraction, Spectroscopy, Reaction yields.

Introduction

The industrial definition of borate is any kind of composition including the boron element. The significance of borates is based on mechanical strength, chemical resistance, electrical and optical features [1, 2]. In metal complexes of borates, each type is preferred in specific applications according to the metal atom in the structure. Zinc borates are commonly used as polymer additive in plastic applications, as an anti-corrosive pigment in paint and automotive industries, as a preservative in wood-based composites and as a flame retardant construction and cement area [3–11]. These applications of zinc borates increased the attention to their synthesis.

Zinc borates can be traditionally prepared in hydrothermal conditions. In the hydrothermal method, the starting materials are dissolved in water separately and the reaction is affected by heat increase and magnetic or mechanic stirring. Different types of zinc borate hydrates may be prepared at different hydrothermal conditions. Schubert et al., synthesized $Zn(B_3O_4(OH)_3)$ at 95°C reaction temperature and 24 hours reaction time [5]. At the same reaction temperature for 8h, $2ZnO \cdot 3B_2O_3 \cdot 3H_2O$ is prepared the using the materials of ZnO and H_3BO_3 [6]. Zheng et al., produced the $4ZnO \cdot B_2O_3 \cdot H_2O$ nano-whiskers using the organic modification agent of phosphate ester [12]. Gao and Liu, synthesized the mixtures of $Zn_2B_6O_{11} \cdot 7H_2O$ and $Zn_3B_8O_{18} \cdot 4H_2O$ at the boiling point of solution using borax and ZnO [13].

The main advantage of ultrasound in hydrothermal synthesis can be explained with the effective interaction of starting materials, and that provides the uniform particle size, shortening in reaction time. As it is seen in literature, the traditional synthesis procedure of zinc borate compounds can be sum up with hydrothermal conditions, reaction times longer than 2 h and modification agents such as oleic acid and polyurethane. For a successful synthesis of zinc, borate has required a minimum of 80°C. As a novel method, the interaction between the raw materials occurs with the impulsion of ultrasound in sonochemical synthesis. The optimum molar ratio of $Zn_5(CO_3)_2 \cdot (OH)_6$ and H_3BO_3, which was determined in the study of Vardar et al. [14], the present study investigates the influence of boron sources on the synthesis of zinc borate compounds. After the synthesis, the samples were characterized by using the techniques of XRD, FT-IR and Raman spectroscopies, therewith surface morphologies and particle sizes were determined by scanning electron microscopy (SEM).

Experimental

Materials

$ZnCl_2$ was purchased from Alfa Aesar as "Zinc chloride anhydrous (98+%, CAS: 7646-85-7)" (Alfa Aesar GmbH & Co KG, Karlsruhe, Germany). H_3BO_3 (Boric acid, 99.9%), $Na_2B_4O_7 \cdot 10H_2O$ (Borax, 99.9%) and $Na_2B_4O_7 \cdot 5H_2O$ (Tincalconite, 99.9%) were

retrieved from Eti Maden - Bandirma Boron Works (Eti Maden, Balikesir, Turkey). NaOH was retrieved from Alfa Aesar as "Sodium hydroxide, pellets, (98%, CAS: 1310-73-2)". Commerical zinc borate seed was obtained from Melos A.Ş. (Melos A.Ş., Istanbul, Turkey). Boron sources were ground by an agate mortar (Retsch RM 100: Retsch GmbH & Co KG, Haan, Germany) to obtain a particle size below 75 μm.

Synthesis procedure

For the determination of the optimum reaction molar ratio of the raw materials, several pre-experiments were conducted. Zn:B (elemental mole to elemental mole) ratio of the raw materials were selected between 1:4 to 1:8 considering the literature reaction schemes [12], which is given in Eqns. (1-3):

$$ZnCl_2 + a(H_3BO_3) + 2NaOH + b(H_2O) \rightarrow$$
$$Zn_3B_6O_{12} \cdot 3.5H_2O + c(H_3BO_3) + 2NaCl + d(H_2O) \quad (1)$$

$$ZnCl_2 + Na_2B_4O_7 \cdot 5H_2O + a(H_3BO_3) + b(H_2O) \rightarrow$$
$$Zn_3B_6O_{12} \cdot 3.5H_2O + c(H_3BO_3) + 2NaCl + d(H_2O) \quad (2)$$

$$ZnCl_2 + Na_2B_4O_7 \cdot 5H_2O + a(H_3BO_3) + b(H_2O) \rightarrow$$
$$Zn_3B_6O_{12} \cdot 3.5H_2O + c(H_3BO_3) + 2NaCl + d(H_2O) \quad (3)$$
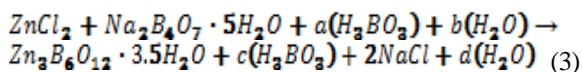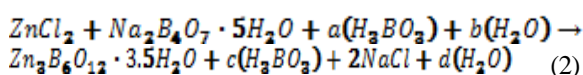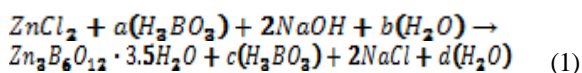
For the synthesis, a 100 mL capacity batch type glass reactor was used with a temperature controller and a cooling jacket. Distilled water obtained from GFL 2004 (Gesellschaft für Labortechnik, Burgwedel, Germany) was used. For the SET-1 synthesis, which the raw materials of H_3BO_3 and NaOH was used at the mole to mole ratio of 1 to 8, 0.1262 moles of H_3BO_3 was put in 25 mL of distilled water and heated to the desired temperature then 0.0158 mole of $ZnCl_2$ and 0.0315 moles of NaOH were added. For the SET-2 synthesis, which the raw materials of $Na_2B_4O_7 \cdot 5H_2O$ and H_3BO_3 were used at the mole to mole ratio of 1 to 8, 0.0715 moles of H_3BO_3 and 0.0179 moles of $Na_2B_4O_7 \cdot 5H_2O$ was put in 25 mL of distilled water and heated to the desired temperature then 0.0179 mole of $ZnCl_2$ were added. For the SET-3 synthesis, which the raw materials of $Na_2B_4O_7 \cdot 10H_2O$ and H_3BO_3 were used at the mole to mole ratio of 1 to 8, 0.0715 moles of H_3BO_3 and 0.0179 moles of $Na_2B_4O_7 \cdot 5H_2O$ was put in 25 mL of distilled water and heated to the desired temperature then 0.0179 mole of $ZnCl_2$ were added. In each set of experiments, for easy crystallization commercial zinc borate seed was added (1% w/w as H_3BO_3 in SET-1, 1% w/w as H_3BO_3 and $Na_2B_4O_7 \cdot 5H_2O$ in SET-2 and 1% w/w as H_3BO_3 and $Na_2B_4O_7 \cdot 10H_2O$ in SET-3).

A Bandelin Sonopuls HD 2070 (20 kHz) model ultrasonic homogenizer (Bandelin electronic GmbH & Co. KG, Berlin, Germany) was used for the synthesis procedure. To investigate the effect of reaction parameters on the synthesized product, the reaction temperatures and reaction times of 80, 85, 90°C and 35, 40, 45, 50 and 55 min were selected, respectively. After the ultrasonic treatment, the solution was filtered with water for the removal of unreacted reactants. The filtrate was dried at 105°C in EcoCELL 111 model oven (MMM Medcenter Einrichtungen GmbH, Planegg, Germany). The reaction procedure was schematized in Fig. 1
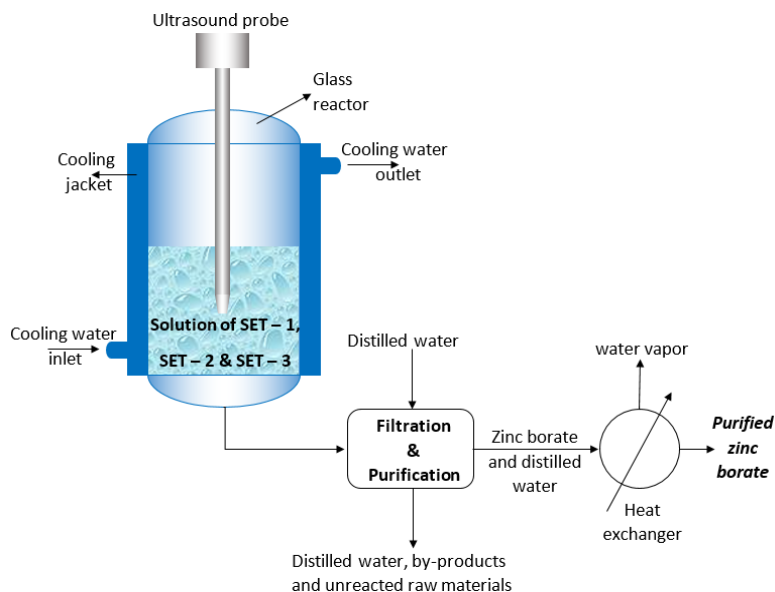
Fig. 1:   Reaction procedure of zinc borate.

Characterizations of the synthesized zinc borates

With the analysis parameters of 40 mA, 45 kV, time step of 0.5 s, step size of 0.03°, scan speed of 0.06°C/s, and 2 theta scan range of 7–90°, sample identifications were carried out by using PANalytical Xpert Pro XRD (PANalytical B.V., Almelo, the Netherlands). For the explanation of patterns, the Inorganic Crystal Structure Database (ICSD) was used. For the characterization of triangular BO_3 and tetrahedral BO_4 bands, FT-IR and Raman spectroscopies were preferred. Perkin Elmer Spectrum One model (PerkinElmer, MA, USA) FT-IR was used with a universal attenuated total reflectance (ATR) sampling accessory (Diamond/Zn). The analysis parameters were set to; resolution 4 cm^{-1}, number of scans 4 and scan range 1800 – 650 cm^{-1}. For the Raman spectroscopy, Perkin Elmer Raman Station 400F (PerkinElmer, CT, USA) model Raman spectrometer was used. The analysis parameters were set to; exposure time 4 s, exposure number 4, data interval 2 cm^{-1} and scan range 1800 – 250 cm^{-1}. Surface morphologies of samples studied by using CamScan Apollo 300 model Field-Emission SEM (CamScan, Oxford, UK). The surface morphologies of the synthesized compounds were investigated at 15 kV with using the backscattered electron (BEI) detector with the magnification of 10000. Thermal behaviour of synthesized phases was characterized by using a Perkin Elmer Diamond TG/DTA with the 10°C/min heating rate in the temperature range of 40–600°C under the nitrogen (N_2) atmosphere.

Reaction efficiency calculation

In the reaction efficiency calculation, three parallel experiments were applied and the average of the repetitions is presented as the results. In the efficiency calculations, $ZnCl_2$ was determined as the limiting reactant. For a batch system, the general reaction yield based on molar flow rates is given in Eqn (4). In here, Y_D is the ratio of the moles of the compound formed at the end of the chemical reaction and N_D is the mole number

of the consumed key reactant. N_{A0} and N_A are the initial and final moles of the key reactant, respectively [15].

$$Y_D = \frac{N_D}{N_{A0} - N_A} \qquad (4)$$

Results and Discussion

XRD results

XRD results for the prepared zinc borates at different (Zn:B) mole ratios were given in Table 1. In here, the XRD score of a compound can be defined with the similarity of the peak intensities (%) and locations of the phase to the pdf card pattern of the reference mineral. According to the results given in Table 1, crystal formation didn't observe at the mole ratios of 1:4 and 1:5 in all of the sets. Also, zinc borate synthesis was only seen at the Zn:B ratios of 1:7 and 1:8 in SET-1. At this Zn:B ratios, higher XRD scores were detected in all sets. This situation indicated that increasing B amount in reaction medium contributed to the zinc borate formation. Major effects of Zn:B mole ratio on the crystal formation of zinc borate structure were seen in SET-2. With the decreasing Zn:B mole ratio, XRD scores of samples were increased dramatically. In SET-3, zinc borate formation began at the mole ratio of 1:6 and minor changes were seen with the increasing B amount. Due to the highest XRD scores for all of the sets, the Zn:B mole ratio of 1:8 was selected as optimum.

Table-1: XRD results of the zinc borates prepared at different (Zn:B) mole ratios.

Zn:B ratio (mole:mole)	SET - 1	SET - 2	SET - 3
1:4	-	-	-
1:5	-	-	-
1:6	-	26*	61
1:7	31*	55	67
1:8	84	92	75

* Partial crystallization

XRD results of the zinc borates prepared at different reaction temperature and time were shown in Table 2. Effects of reaction temperature and time examined in the range of 80 – 90°C and 35 – 55 minutes, respectively.

Table-2: XRD results of the zinc borates prepared at different reaction temperature and time.

Reaction temperature (°C)	Reaction time (min)	SET - 1	SET - 2	SET - 3
90	55	84	92	75
	50	77	87	70
	45	68	84	54*
	40	63	77	35*
	35	-	26*	-
85	55	81	91	74
	50	76	81	64
	45	63	65	37*
	40	58	38*	34*
	35	-	-	-
80	55	80	30*	45*
	50	75	26*	30*
	45	-	22*	25*
	40	-	-	-
	35	-	-	-

* Partial crystallization

The results indicated that the reaction times of 35 and 40 minutes at lower temperatures were not suitable for the complete crystalline zinc borate formation. In Set-1, in 90°C and 85°C at 35 min reaction time and 80°C at below 50 min reaction time obtained zinc borate phases were completely amorphous. In Set-2, in 90°C at 35 min reaction time, in 85°C at 40 min reaction time and in 80°C at between 55 and 35 min reaction time the obtained phases are partially amorphous hence both crystal and amorphous formations have occurred. Also in Set-2 in 85°C at 35 min reaction time and 80°C at below 45 min reaction time obtained zinc borate phases were completely amorphous. In Set-3, in 90°C at between 45 and 40 min reaction time, in 85°C at between 45 and 40 min reaction time and in 80°C at between 55 and 45 min reaction time the obtained phases are partially amorphous. In Set-3 complete amorphous phases were seen in 90°C and 85°C at 35 min reaction time, in 80°C at between 40 and 35 min reaction time. In the selected ranges of reaction temperature and time, it was seen that the increases in reaction temperature contributed to the lessening reaction time to zinc borate synthesis. The desired crystal formation can be seen at the longer reaction times of 45 minutes.

Generally, higher XRD scores were obtained at SET-2 and this proved that the tincalconite can be a suitable boron source for the zinc borate synthesis. All of the sets, the highest XRD scores were obtained at the reaction temperature of 90°C and the reaction time of 55 minutes. XRD patterns of samples prepared at these conditions were presented in Fig 2. The obtained characteristic peaks in XRD analyses were in good agreement with the literature [16-18].
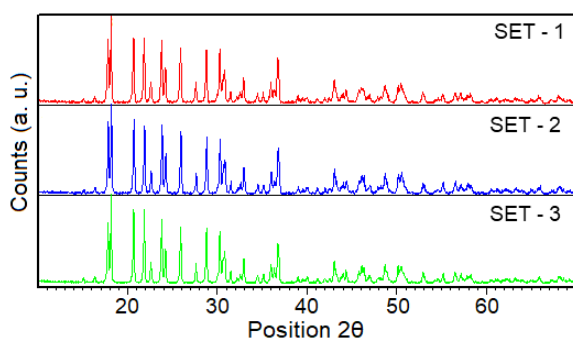
Fig. 2:   XRD patterns of the optimum samples for each set.

Spectroscopic results

FT-IR and Raman analysis were applied to the highest obtained XRD scored products and are given in Fig 3 and Fig 4, respectively. From the FT-IR spectra,

the bands between 1467 and 1252 cm^{-1} could be explained as the $v_{as}(B_{(3)}$-O) (asymmetric stretching of the three-coordinate boron to oxygen) The bands between 1188 to 1109 cm^{-1} could be ascribed as δ(B-O-H) (the bending of boron-oxygen-hydrogen). $v_{as}(B_{(4)}$-O) (asymmetric stretching of the four-coordinate boron to oxygen bands was obtained at between 1061–1060 cm^{-1}. $v_s(B_{(3)}$-O) (symmetric stretching of three-coordinate boron to oxygen) bands were seen between 921 – 917 cm^{-1}. The bands between 856 – 792 cm^{-1} could be described as $v_s(B_{(4)}$-O) (symmetric stretching of four-coordinate boron to oxygen). The stretching of $v_p(B(OH)_4)^-$ was obtained at the band values between 750 – 749 cm^{-1}. Lastly, $\gamma(B_{(3)}$-O) (bending of the three-coordinate boron to oxygen) was identified at 674 cm^{-1}. Obtained bands were in good agreement with the literature [19, 20].

In the Raman spectra, bands in the range of 1291 – 1293 cm^{-1} indicated the stretching of $v_{as}(B_{(3)}$–O). $v_{as}(B_{(4)}$–O) and δ(B–O–H) were seen at 1049 cm^{-1} and between 1191 and 1188 cm^{-1}, respectively. The peak values between at 849 and 755 cm^{-1} correspond to the stretching of $v_s(B_{(4)}$–O). $\gamma(B_{(3)}$–O) stretching was seen between 665 and 664 cm^{-1}. The band around to 578 cm^{-1} can be explained with the $\delta(B_{(3)}$–O)/$\delta(B_{(4)}$–O) stretching. The last region, which indicates to the stretching of $\delta(B_{(4)}$–O), were between 437 and 298 cm^{-1}. Obtained bands were in good agreement with the literature [21, 22].
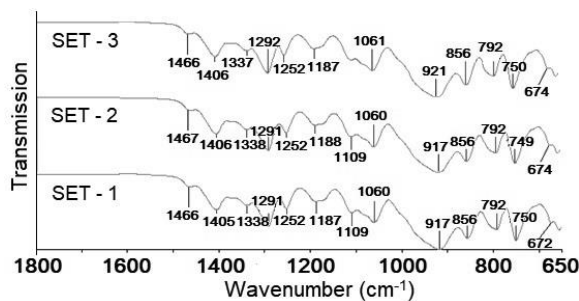
Fig. 3:   FT-IR spectra of the optimum products
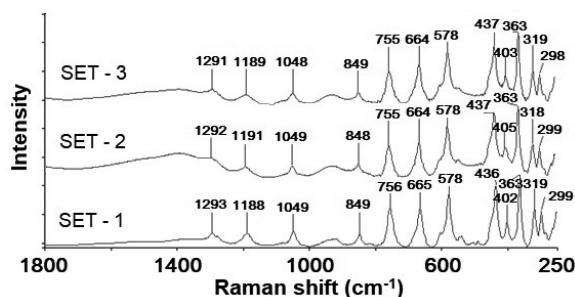
Fig. 4:   Raman spectra of the optimum products.

SEM results

The particle shape of zinc borates can be effected from the parameter changes in reaction conditions. [23]. Hexahedral and polyhedral particles were observed with the effects of the ultrasonic effect. The SEM morphologies of the selected as optimum particles were given in Fig 5. According to the analysis results for SET-1, different shapes of sharp particles were obtained. The particle sizes varied between 1.3 μm and 440 nm for SET-1. The hexahedral particles at homogeneous distribution were seen in SET-2. The smallest particles were determined in the reaction of tincalconite and zinc chloride (SET-2) and the particle sizes were changed in the range of 504 – 172 nm. In the reaction of borax and zinc chloride (SET-3), the well-dispersed polyhedral and elliptic particle in the particle sizes of 855-189 nm.

Reaction efficiencies

The reaction efficiencies calculated using Eqn. 4, are given in Fig 6. According to the results with the increase in reaction time and reaction temperature, the reaction efficiencies increased. Obtained reaction efficiencies were calculated between 79.6 - 86.2%, 85.1 – 89.2% and 83.0 – 94.0% for SET-1, SET-2 and SET-3, respectively. The highest reaction efficiencies were calculated at the reaction temperature of 90°C and at the reaction time of 55 min. The lowest reaction efficiencies were observed at the experimental 1st set-up, and the highest reaction efficiencies were observed at the experimental 3rd set-up of experiments. All reaction efficiencies were calculated within 0.5% experimental error.
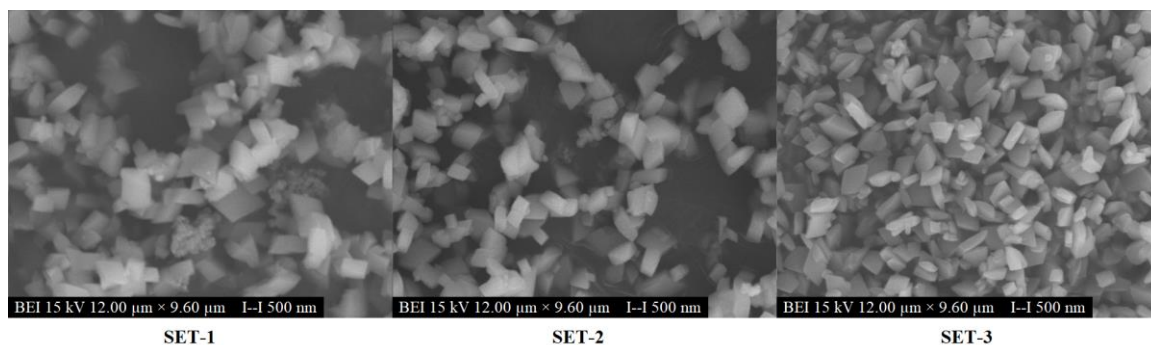
Fig. 5: SEM morphologies of the synthesized optimum zinc borate compounds.
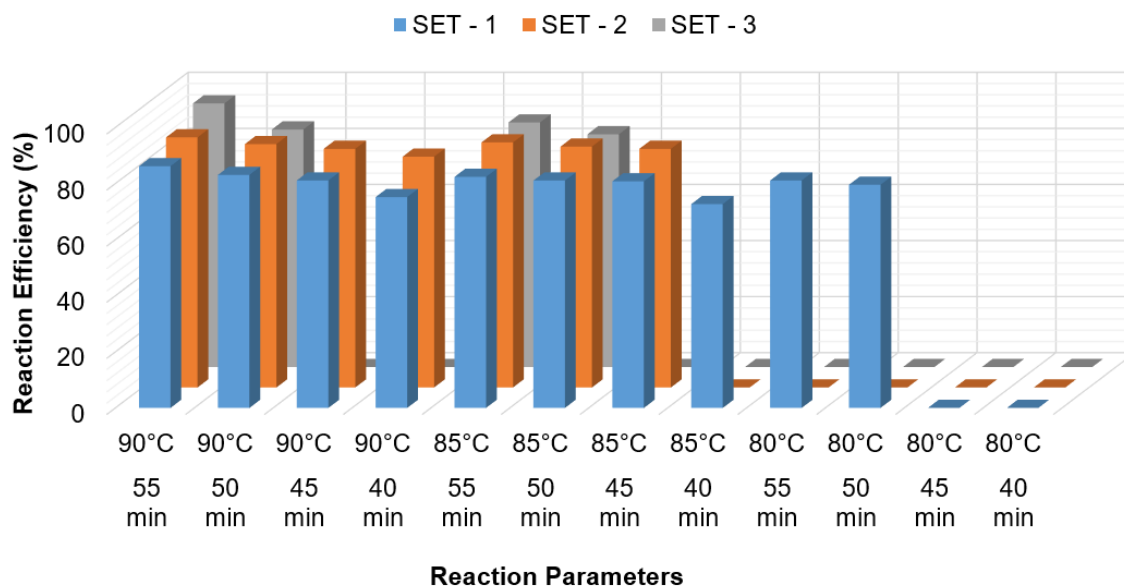
Fig. 6: The reaction efficiencies of the synthesized zinc borate compounds.
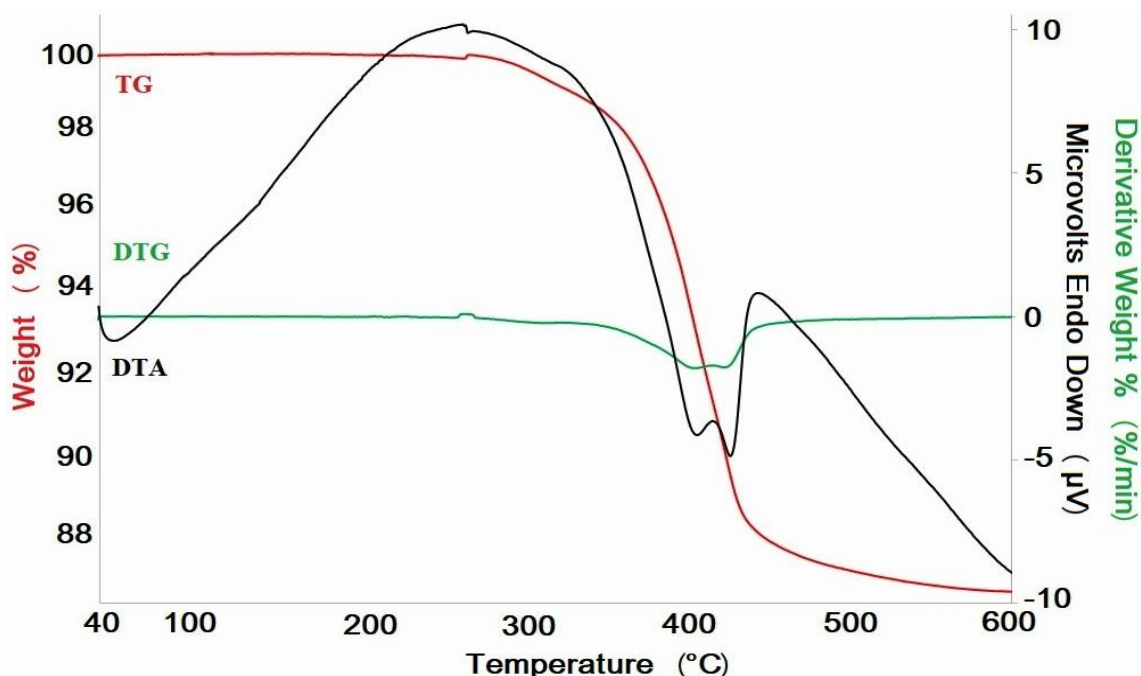
Fig. 7:   Thermal analysis result of synthesized $Zn_3B_6O_{12} \cdot 3.5H_2O$.

In the literature, the hydrothermal synthesis without ultrasound of zinc borates were studied and the reaction efficiencies were found within the range of; 88.10-96.10% at 70-90°C and 120-180 min of reaction time from the raw materials of $ZnSO_4 \cdot 7H_2O$-NaOH-H_3BO_3 [16]; 86.50-97.80% at 70-90°C and 120-240 min of reaction time from the raw materials of $ZnCl_2$-NaOH-H_3BO_3 [16]; 86.50-99.60% at 70-90°C and 180-240 min of reaction time from the raw materials of $ZnSO_4 \cdot 7H_2O$-$Na_2B_4O_7 \cdot 5H_2O$-H_3BO_3 [17]; 86.20-87.70% at 120 min of reaction time from the raw materials of $ZnCl_2$-$Na_2B_4O_7 \cdot 5H_2O$-H_3BO_3 [17]. As it is seen that by using the $ZnCl_2$ as a starting material in the ultrasonic synthesis of zinc borates the reaction efficiencies were increased at some parameters with the obvious decrease in the reaction times.

Thermogravimetric results

Thermal curves of synthesized $Zn_3B_6O_{12} \cdot 3.5H_2O$ were presented in Fig 7. As it is seen in the thermal analyses results of zinc borate hydrate, the compound lost its hydrate molecules in a two-step reaction. According to the TG and DTG curves, The first step occurs in the range of 262 – 413°C and the mass loss was 8.10%. The second step begins at the end of the first step and the removal of hydrate molecules were continue until 610°C. The mass loss was determined as 5.15% for the second step of dehydration. The endothermic peaks of DTA were seen at 403°C and 425°C for the first and second steps of dehydration, respectively.

The obtained temperature ranges for each step and total mass loss of 13.25% is consistent with the thermal studies on zinc borate hydrates [16].

Conclusions

In this research, the synthesis of a zinc borate compound of $Zn_3B_6O_{12} \cdot 3.5H_2O$ is prepared from different boron sources via a novel green method of ultrasound-assisted. For each boron source, an experimental plan was created. Several reaction temperatures ranging from 80 - 90°C and reaction times 40 – 55 min were selected for the determination of best formation. This characterization study indicates a significant contribution of raw material selection on the characteristic properties of synthesized sample. The use of zinc chloride in ultrasound-assisted synthesis is also effective on the basis of the reaction yield in comparison with the literature [16, 17]. Homogeneous hexahedral particles at higher XRD scores were obtained with the particle sizes between 77 – 296 nm in SET-2. The obtained spectra of both FT-IR and Raman were in good agreement with the literature. The decomposition of prepared hydrated compound emerges in the range of 262 – 610°C with a two-step reaction.

The obtained results would prepare a substructure for the ultrasound applications of new borate compounds and boron technology.

References

1. R. Adair, *Boron*, The Rosen Publishing Group, Inc, New York, (2007)
2. C. Helvaci and M.R. Palmer, Origin and Distribution of Evaporite Borates: The Primary Economic Sources of Boron, *Elements* **13**, 249 (2017).
3. D. Gurhan, G.O. Cakal, I. Eroglu and S. Ozkar, Improved synthesis of fine zinc borate particles using seed crystals, *J. Cryst. Growth.* **311**, 1545 (2009).
4. Y. Tian, Y. He, L. Yu, Y. Deng, Y. Zheng, F. Sun, Z. Liu and Z. Wang, In situ and one-step synthesis of hydrophobic zinc borate nanoplatelets, *Colloid. Surface. A.*, **312**, 99 (2008).
5. D. Schubert, F. Alam, M. Visi and C. Knobler, Structural Characterization and Chemistry of the Industrially Important Zinc Borate, $Zn[B_3O_4(OH)_3]$, *Chem. Mater.* **15**, 866 (2002).
6. X. Shi, Y. Xiao, M. Li, L. Yuan and J. Sun, Synthesis of an industrially important zinc borate, $2ZnO \cdot 3B_2O_3 \cdot 3H_2O$, by a rheological phase reaction method, *Powder Technol.* **186**, 263 (2008).
7. Genovese and R.A. Shanks, Structural and thermal interpretation of the synergy and interactions between the fire retardants magnesium hydroxide and zinc borate, *Polym. Degrad. Stabil.* **92**, 2 (2007).
8. Yildiz, M.O. Seydibeyoglu and F.S. Guner, Polyurethane–zinc borate composites with high oxidative stability and flame retardancy, *Polym. Degrad. Stabil.* **94**, 1072 (2009).
9. C.A. Giudice and J.C. Benitez, Zinc borates as flame-retardant pigments in chlorine-containing coatings, *Prog. Org. Coat.* **42**, 82 (2001).
10. M.S. Gaafar, N.S. Abd El-Aal and O.W. Gerges, G. El-Amir, Elastic properties and structural studies on some zinc-borate glasses derived from ultrasonic, FT-IR and X-ray techniques, *J. Alloy. Compd.* **475**, 535 (2009).
11. B. Garba, Effect of zinc borate as flame retardant formulation on some tropical woods, *Polym. Degrad. Stabil.*, **64**, 517 (1999).
12. Y. Zheng, Y. Tian, H. Ma, Y. Qu, Z. Wang, D. An, S. Guan and X. Gao, Synthesis and performance study of zinc borate nanowhiskers, *Colloid. Surrface. A.*, **339**, 178 (2009).
13. Y.H. Gao and Z.H. Liu, Synthesis and thermochemistry of two zinc borates, $Zn_2B_6O_{11} \cdot 7H_2O$ and $Zn_3B_{10}O_{18} \cdot 14H_2O$, *Thermochim Acta,.* **484**, 27 (2009).
14. D.S. Vardar, A.S. Kipcak, F.T. Senberber, E.M. Derun, N. Tugrul and S. Piskin, Zinc Borate Synthesis Using Hydrozincite and Boric Acid with Ultrasonic Method, *International Scholarly and Scientific Research and Innovation,* **9,** 1287 (2015).
15. H.S. Fogler, *Element of Chemical Reaction Engineering*, 3rd edn, Prentice-Hall, New Jersey, (1999).
16. A.S. Kipcak, F.T. Senberber, E.M. Derun, N. Tugrul and S. Piskin, Characterization and thermal dehydration kinetics of zinc borates synthesized from zinc sulfate and zinc chloride, *Res. Chem. Intermediat.*, **41,** 9129 (2015).
17. A.S. Kipcak, F.T. Senberber, M. Yildirim, S.A. Yuksel, E.M. Derun and N. Tugrul, Characterization and physical properties of hydrated zinc borates synthesized from sodium borates, *Main Group Metal Chem.*, **39**, 59 (2016).
18. M. Bardakci, N.B. Acarali, N. Tugrul, E.M. Derun, M.B. Piskin, Production of Zinc Borate for Pilot Scale Equipment and Effects of Reaction Conditions on Yield, *Mater. Sci. Medzg.*, **19**, 158 (2013).
19. J. Yongzhong, G. Shiyang, X. Shuping and L. Jun, FT-IR spectroscopy of supersaturated aqueous solutions of magnesium borate, *Spectrochim Acta A*, **56**, 1291 (2000).
20. O. Akgul, N.B. Acarali, N. Tugrul, E.M. Derun and S. Piskin, X-Ray Thermal FT-IR and Morphological Studies of Zinc Borate in Presence of Boric Acid Synthesized by Ulexide Mineral, *Period. Mineral.*, **83**, 77 (2014).
21. S. Li, D. Xu, H. Shen, J. Zhou and Y. Fan, Synthesis and Raman properties of magnesium borate micro/nanorods, *Mater. Res. Bull.*, **47**, 3650 (2012).
22. A.S. Kipcak, N.B. Acarali, F.T. Senberber, M. Yildirim, S.N.T. Koc, S.A. Yuksel, M.B. Piskin, E.M. Derun and N. Tugrul, Synthesis of Dehydrated Zinc Borates using the Solid State Method and Characterization and Investigation of the Physical Properties, *Main Group Chem.*, **15**, 301 (2016).
23. P. Liang, Z. Tuoheti and Z.H. Liu, Controlling the structure and morphology of zinc borate by adjusting the reaction temperature and pH value: formation mechanisms and luminescent properties, *RSC Adv.*, **7,** 3695 (2017).